Hindawi
Geofluids
Volume 2020, Article ID 8876099, 8 pages
https://doi.org/10.1155/2020/8876099

Research Article

The Loading Rate Effect on the Fracture Toughness of Marble Using Semicircular Bend Specimens

Fengqiang Gong,[1,2,3] **Yunliang Wang**,[3] **and Shanyong Wang**[4]

[1]*Engineering Research Center of Safety and Protection of Explosion & Impact of Ministry of Education (ERCSPEIME), Southeast University, Nanjing 211189, China*
[2]*School of Civil Engineering, Southeast University, Nanjing 211189, China*
[3]*School of Resources and Safety Engineering, Central South University, Changsha 410083, China*
[4]*ARC Centre of Excellence for Geotechnical Science and Engineering, Faculty of Engineering and Built Environment, The University of Newcastle, University Drive Callaghan, NSW 2308, Australia*

Correspondence should be addressed to Fengqiang Gong; fengqiangg@126.com

Received 13 August 2020; Revised 13 September 2020; Accepted 24 September 2020; Published 13 October 2020

Academic Editor: Zhijie Wen

A series of dynamic fracture experiments on semicircular bend (SCB) marble specimens were conducted to characterize the loading rate effect using the INSTRON testing machine and the modified SHPB testing system. The fracture toughness of the marble specimens was measured from a low loading rate to a high loading rate (10^{-3}~10^{6} MPa·m$^{1/2}$s^{-1}). The results show that the fracture toughness will increase with the loading rate. Since the fracture toughness at a magnitude of 10^{-3} MPa·m$^{1/2}$s^{-1} is regarded as the static fracture toughness, the specific value of DIF_f (the dynamic increase factor of fracture toughness) can be obtained at the other loading magnitudes from dynamic fracture tests. To describe the variation in DIF_f from low to high loading rates, a new continuous model of DIF_f was put forward to express the quantitative relation between the loading rate and rock dynamic fracture toughness. It is shown that the new DIF_f model can accurately describe the loading rate effect on the dynamic fracture testing data for rock materials.

1. Introduction

The failure of rock or rock mass, such as rock cutting, hydraulic fracturing, rock burst, and spalling, is closely related to the initiation and propagation of internal cracks under complex stress [1–6]. This phenomenon has been observed in many laboratory tests or engineering sites [7–10]. Fracture mechanics plays a crucial role in geophysical processes and engineering applications involving rock or underground engineering [11–14]. Rock fracture toughness, as an intrinsic material property of rocks, is considered an important factor for resisting crack initiation and propagation and thus has been widely investigated in the rock mechanics community [15–17]. Accurate measurement of fracture toughness is critical for understanding rock fracture mechanisms and solving engineering problems.

Many methods have been proposed to measure the fracture toughness of brittle materials such as rocks. For example, short rod (SR) and chevron bending (CB) tests in 1988 [18], the cracked chevron-notched Brazilian disc (CCNBD) testing in 1995 [19], and chevron-notched SCB testing [20]. The Brazilian disc test [21] was proposed by the International Society for Rock Mechanics (ISRM) as a method for rock fracture testing. In addition, cracked straight through Brazilian disk (CSTBD) tests [22, 23] are also often used to measure fracture toughness. In addition, the semicircular bend (SCB) was proposed in 1984 by Chong and Kuruppu [24], and the geometry of the sample is convenient for sample processing (directly from rock cores) and experimentation. The ISRM recently adopted the semicircular bend (SCB) method for characterizing the static and dynamic mode I fracture toughness of rocks [25, 26]. Thus, this method is used for static and

(a) (b)

Figure 1: (a) Cored rock and (b) SCB specimen.

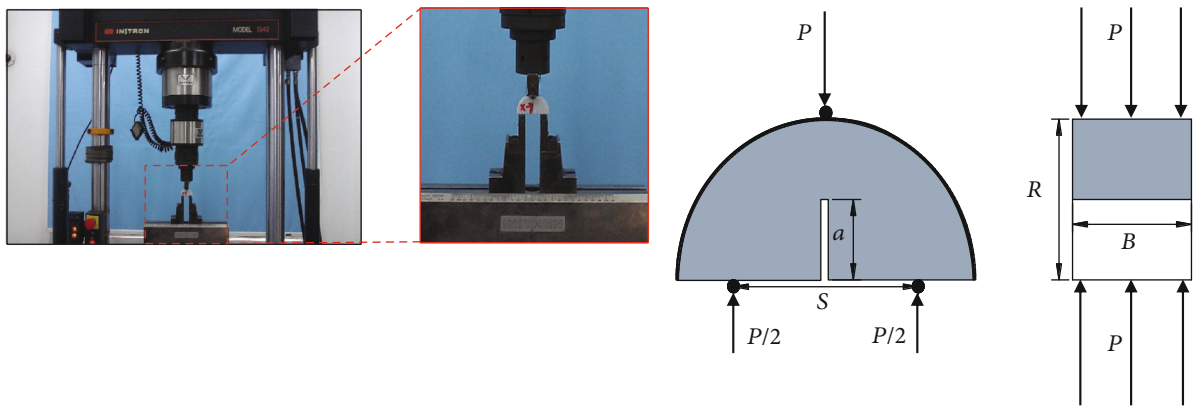

(a) (b)

Figure 2: (a) INSTRON testing system and (b) SCB specimen geometry and schematic loading arrangement.

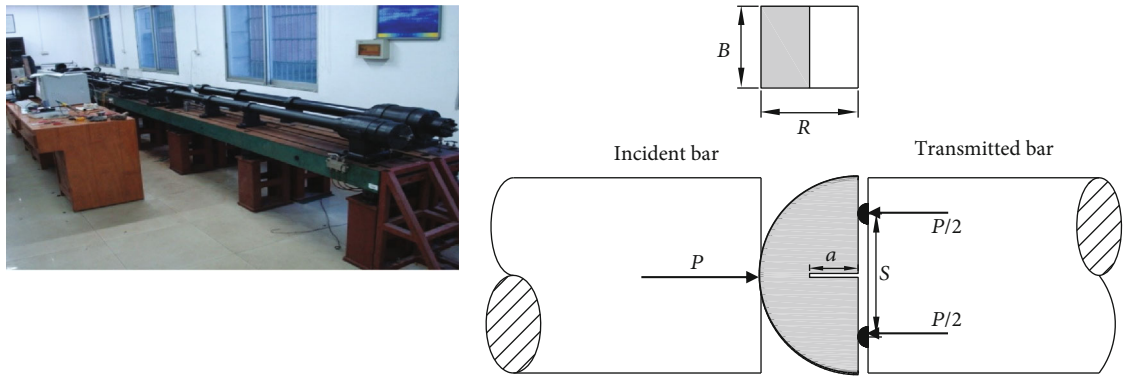

(a) (b)

Figure 3: (a) SHPB system for rock dynamic fracture testing. (b) Schematics of the semicircular bend (SCB) specimen in the split Hopkinson pressure bar (SHPB) system.

dynamic fracture experiments, and a large number of experimental results have shown that the loading rate has an important influence on the mechanical properties of rock [27, 28].

Existing attempts to measure rock fracture toughness were mostly conducted under limited dynamic loading by using a split Hopkinson pressure bar (SHPB) [29, 30]. Limited attempts have been made to study the static and dynamic fracture toughness of rocks simultaneously. Zhang and Zhao [31] studied the effect of the loading rate on the fracture toughness and failure micromechanisms in marble. Zhang et al. [27] measured the fracture toughness of marble for a wide range of loading rates from 10^{-2} MPa·m$^{1/2}$s^{-1} to 10^{6} MPa·m$^{1/2}$s^{-1}. Backersa et al. [32] investigated the influence of the loading rate on the fracture toughness of sandstone samples subjected to mode I loading and noted that at low velocities, the fracture toughness remains approximately constant. By exceeding a fracture velocity threshold, the fracture toughness increases significantly. All the above research shows the following conditions: (1) Although many people have studied SCB testing, most only consider the dynamic loading range and obtain the rate effect of fracture

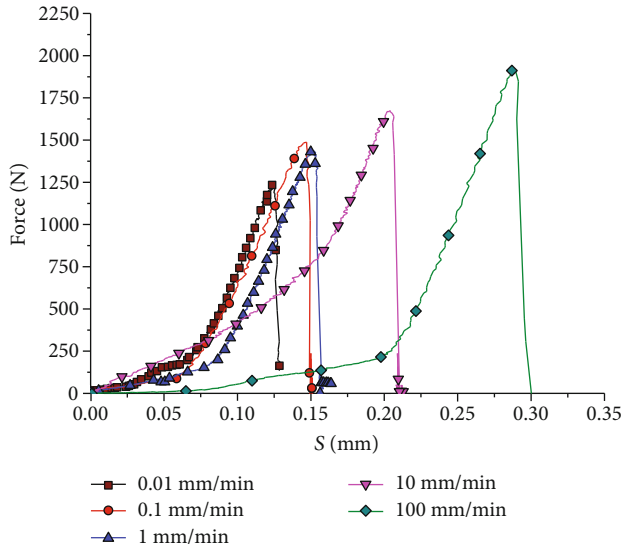

Figure 4: Load-displacement curves during the fracture tests for different loading rates.

toughness. Therefore, the wide ranges of loading rates have not been investigated by SCB testing at present. (2) There is no description of the normalized model for the dynamic increase factor available from low loading rates to high loading rates.

In this study, the semicircular bend (SCB) test was conducted on marble using a servo-hydraulic testing machine and a modified SHPB system. Then, the change rule of the fracture toughness of rock with the loading rate was obtained. Based on this result, at a wide range of low to high loading rates, a new continuous model of DIF_f for the rock dynamic fracture was put forward to express the quantitative relation between the loading rate and dynamic fracture toughness.

2. SCB Specimen Preparation

To investigate the fracture properties of the rock material, marble [15, 16] extracted from Leiyang in Hunan Province was chosen as the experiment material. According to the suggested method of specimen processing for SCB testing [24], marble cores with 50 mm diameters were first drilled from a rock block and then sliced to obtain discs with thickness of 20 mm. The surface roughness of all the specimens is less than 0.5% of the thickness. Then, SCB specimens were machined from the obtained discs by radial cutting; i.e., a notch with a width of approximately 1 mm was subsequently processed with a 0.5 mm thick hacksaw blade by radial cutting from the centre of the disc. In addition, sufficient crack tip sharpness is necessary for accurately measuring the fracture initiation toughness. The specimen processing is shown in Figure 1.

3. Experimental Setup

The INSTRON testing system (Figure 2) from the modern analysis and testing centre of Central South University was employed to perform the static measurement of fracture toughness. The test results were collected by a computer. The INSTRON testing system is shown in Figure 2(a). In addition, the SCB specimen geometry and schematic loading arrangement are shown in Figure 2(b), in which the specimen was loaded by a three-point bending fixture.

A constant loading rate of 4 kN/min was applied by displacement control during the experiments. The specimen was loaded at the constant rate until it was totally fractured. This relatively low loading rate is not only conducive to the stable development of a surface crack and nonlinear fracture process zone at a crack tip but also convenient to measure the fracture toughness. The SHPB system is often used to test various dynamic parameters of rock materials [33–36]. In these tests, the dynamic fracture testing of the rock was conducted using a 50 mm diameter SHPB system (see Figure 3), which has been used in many dynamic tests [37, 38]. c mm; this apparatus can simulate pulse waveforms to reduce high-frequency vibration and minimize the dispersion degree of the test results. This system also includes an incident bar 2000 mm in length and a transmission bar 1500 mm in length. To carry out the tests, the specimens were clamped between the incident and transmitted bars. In addition, before the tests, the longitudinal wave velocity of the marble was measured, and its minimum value is 3.09 km/s.

4. Formula

The initiation fracture toughness K_{IC} of SCB is determined by the ISRM-suggested method [24]:

$$K_{IC} = \frac{P_{max}\sqrt{\pi a}}{2RB} Y', \tag{1}$$

$$Y' = -1.297 + 9.516\left(\frac{S}{2R}\right) - \left(0.47 + 16.457\left(\frac{s}{2R}\right)\right)\beta + \left(1.071 + 34.401\left(\frac{s}{2R}\right)\right)\beta^2, \tag{2}$$

$$\beta = \frac{a}{R}, \tag{3}$$

where P_{max} is the measured peak load at specimen failure; R and B are the radius and the thickness of the specimen, respectively; A is the prefabricated crack length; Y' is the minimum dimensionless stress intensity factor; and S is the length of the load end. In this work, the standard sizes mentioned in the literature are used as follows [25]:$S/2R = 0.667$ and $a/R = 0.2$. According to the principle of SHPB in dynamic fracture testing, the specific value of the dynamic fracture toughness can be calculated by substituting P_{max} into Equation (1).

In the test of the SCB mode I fracture toughness, the loading rate of the test was defined as the rate of change in the stress intensity factor at the crack tip ($\dot{K}_{Id}$) because $\dot{K}_{Id}$ can accurately respond to the rate of change in the stress field during the loading process. The dynamic loading rate can

Table 1: Fracture test results of rock specimens under the quasistatic load.

No.	Control rate (mm/min)	t (s)	Log time	Fracture toughness (MPa·m$^{0.5}$)	Loading rate (MPa·m$^{0.5}$s^{-1})	Log loading rate
S-2	0.01	566	2.7528	0.5407	0.0010	-3.0199
S-3	0.01	781	2.8927	0.5379	0.0007	-3.1620
S-6	0.01	745	2.8722	0.5748	0.0008	-3.1126
S-7	0.1	212	2.3263	0.6434	0.0030	-2.5178
S-8	0.1	131	2.1173	0.7228	0.0055	-2.2582
S-9	0.1	88	1.9445	0.6820	0.0077	-2.1107
S-10	1	6.00	0.7782	0.6465	0.1078	-0.9676
S-11	1	5.75	0.7597	0.6533	0.1136	-0.9446
S-1	1	8.91	0.9498	0.6625	0.0744	-1.1286
S-13	10	1.1656	0.0665	0.6810	0.5842	-0.2334
S-14	10	1.2346	0.0915	0.7575	0.6135	-0.2122
S-15	10	1.3326	0.1247	0.7105	0.5332	-0.2731
S-16	100	0.1426	-0.8459	0.8788	6.1627	0.7898
S-17	100	0.1836	-0.7361	0.9317	5.0746	0.7054
S-18	100	0.1706	-0.7680	0.8108	4.7526	0.6769

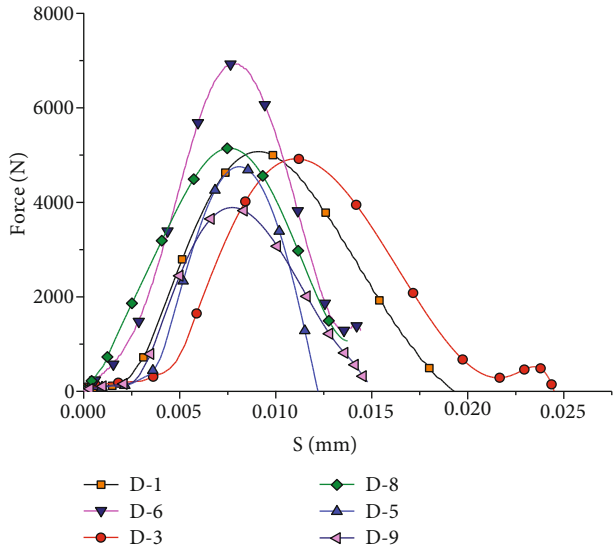

Figure 5: Load-displacement curves of different loading rates.

be calculated according to the following equation:

$$\dot{K}_{\mathrm{Id}} = \frac{K_{\mathrm{Id}}}{t_f}, \tag{4}$$

where K_{Id} refers to the dynamic fracture toughness and t_f is the time needed for the main crack to run through the entire specimen.

5. Experimental Results

5.1. Quasistatic Fracture Test Results at a Low Loading Rate. To analyse the relationship between the load and the displacement of the fracture under a quasistatic load, the load-displacement curves of the specimens under different loading rates during the fracture tests are shown in Figure 4. From Figure 4, it appears that the fracture process of a specimen can be divided into two distinct phases, i.e., the steady increase phase and the sharp increase phase. Between these two phases, a turning point is clearly observed. After entering the sharp increase phase, the specimen is in a relatively stable loading process; near the fracture point, the specimen suddenly brakes, leading to destruction. During the initial loading stage, some microcracks existing in the rock closed, which caused larger deformation under a lower load, i.e., the steady increase phase. With the load increasing, the new microcracks developed and extended, which led to the sharp increase phase. The fracture test results of rock specimens under the quasistatic load are summarized in Table 1.

The results show that the fracture toughness of rock changes with the increase in the loading rate under quasistatic loading. The fracture toughness increases with the loading rate, and the maximum value of the fracture toughness is 0.9317 MPa·m$^{0.5}$, which is an increase of approximately 72% compared with the minimum fracture toughness of 0.5407 MPa·m$^{0.5}$. According to the traditional method, a linear function was used to express the relationship between the loading rate and fracture toughness.

5.2. Fracture Test Results of Rock under Dynamic Loading. The relationship between the load and the displacement of the fracture under a dynamic load in the SHPB test, as illustrated in Figure 5, is analysed here. The results of the rock dynamic fracture tests are also shown in Table 2.

It appears that the load-displacement curve of the specimen during the dynamic fracture process has a similar change rule to that in the static state; the fracture process can clearly be divided into a steady increase phase and a sharp increase phase. Relative to the curve under a static state, the steady increase phase during the dynamic fracture process is shorter and the proportion of the sharp increase phase tends to increase. This may be caused by the different dynamic responses of the rock materials under impact

Table 2: The results of the rock dynamic fracture tests under dynamic loading.

No.	t (s)	Log time	Fracture toughness (MPa·m$^{0.5}$)	Loading rate (MPa·m$^{0.5}$s^{-1})	Loading rate log
D-1	0.000092	-4.0362	2.2916	24908.9586	4.3964
D-3	0.000100	-4.0000	2.3858	23858.1967	4.3776
D-5	0.000103	-3.9872	2.3188	22513.0907	4.3524
D-6	0.000101	-3.9957	3.4986	34639.4462	4.5396
D-8	0.000102	-3.9914	2.4494	24014.1115	4.3805
D-9	0.000089	-4.0506	1.8268	20525.4466	4.3123
B-1	0.000044	1.64345	7.1655	162853.964	5.2117
B-2	0.000047	1.67209	3.0971	65896.6140	4.8188
B-3	0.000043	1.633468	6.1324	142614.663	5.1541
B-4	0.000050	1.69897	4.3066	86133.5032	4.9351
B-6	0.000072	1.85733	3.6652	50906.3257	4.7067

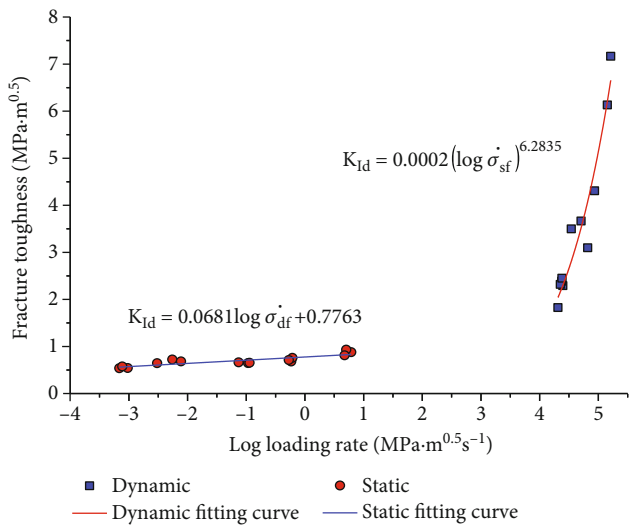

Figure 6: Comparison of the fracture toughness under dynamic and static loading.

loading. In addition, the failure displacement of a specimen under dynamic loading is clearly smaller than that of a specimen under static loading. This is because the dynamic impact speed is very high, causing the crack to rapidly develop through the specimen, and the failure of a specimen produces relatively less deformation.

The relationship between the fracture toughness and logarithm of the loading rate is shown in Figure 6. From the scatter diagrams in Figure 6, it appears that the marble fracture toughness under dynamic loading was significantly higher than that under a static condition and follows a similar increasing trend with the increase in the loading rate [28].

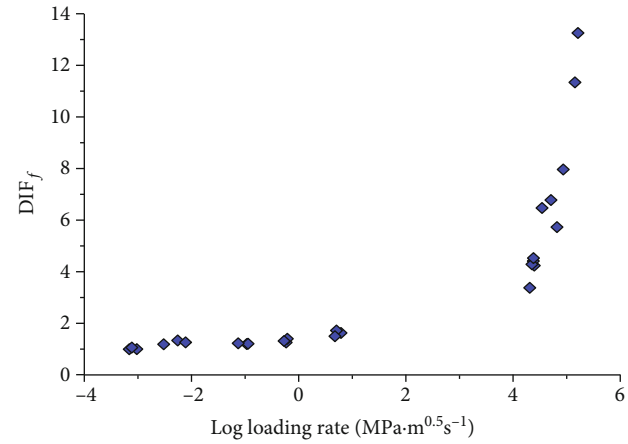

Figure 7: Comparison of the fitting formula and measured data.

The maximum value of the fracture toughness is 7.1655 MPa·m$^{0.5}$, which is an increase of approximately 292% from the minimum fracture toughness of 1.8268 MPa·m$^{0.5}$; the loading rate effect is much more apparent.

Based on the above research results, it can be concluded that a clear loading rate effect exists for the fracture toughness of marble. Both the fracture toughness at a low loading rate and a high loading rate are logarithmically increased as the loading rate increases, but their growth trends are different. It can be seen from Figure 7 that at low loading rates, the marble fracture toughness and the loading rate (logarithmic) show a linear but relatively slow increase. At high loading rates, the marble fracture toughness increases rapidly with the increase in the loading rate (logarithmic), and these parameters are related. Their relationships can be expressed by the following equations:

(i) Low loading rate:

$$K_{Id} = 0.0681 \log \dot{\sigma}_{df} + 0.7763, \quad (5)$$

(ii) High loading rate:

$$K_{Id} = 0.0002(\log \dot{\sigma}_{sf})^{6.2835}, \quad (6)$$

where K_{Id} is the fracture toughness under different loading rates, $\dot{\sigma}_{df}$ is the loading rate of the dynamic fracture, and $\dot{\sigma}_{sf}$ is the static fracture loading rate.

6. Discussion

Most of the existing studies on the normalized model of the dynamic increase factor have focused on compression or tensile tests. Additionally, the dynamic increase factor is usually divided: one function is used for low loading rates and another function is used for high loading rates. Over the past

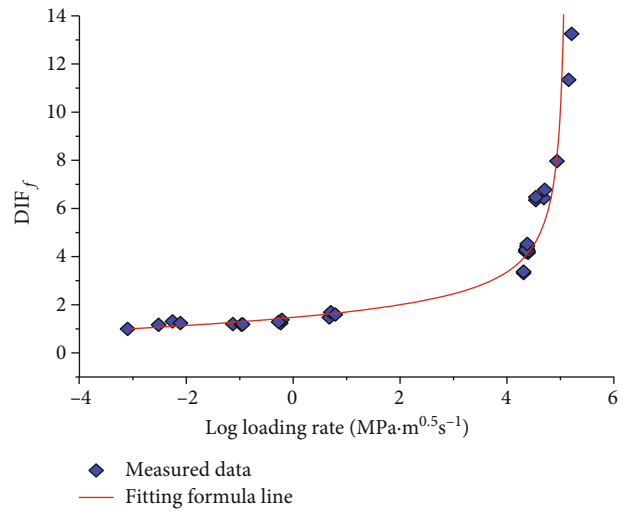

Figure 8: Variation in the rock fracture toughness at low to high loading rates.

decades, the normalized dynamic uniaxial compressive strength has been obtained as a function of the strain rate [39, 40], and the normalized dynamic tensile strength [41, 42] has been obtained as a function of the loading rate. Thus, the accurate determination of the normalized model of the dynamic increase factor is crucial for understanding the fracture mechanisms over a wide range of loading rates and is beneficial for engineering applications.

The DIF_f (DIF of fracture toughness) was proposed to compare the trend of the change in the fracture toughness for a range of low and high loading rates. In addition, DIF_f can be expressed as follows:

$$\mathrm{DIF}_f = \frac{K_{\mathrm{Id}}}{K_{\mathrm{Is}}}, \tag{7}$$

where K_{Id} is the fracture toughness under different loading rates and K_{Is} is the fracture toughness under the minimum loading rate. The DIF_f test results under medium-low loading rates and high loading rates are plotted in Figure 8.

As mentioned previously, traditional analysis methods are generally used to separate the results of the medium-low loading rates and high loading rates. Therefore, according to the latest research results from Gong and Zhao [43], a unified expression for the relationship between the fracture toughness and the loading rate of rock for all the loading rates is presented. The expression of the fitting function is as follows:

$$\mathrm{DIF}_f = \left(\frac{\alpha}{\alpha - \log\left(\dot{\sigma}_{\mathrm{df}}/\dot{\sigma}_{\mathrm{sf}}\right)}\right)^{1-\beta(\log\left(\dot{\sigma}_{\mathrm{df}}/\dot{\sigma}_{\mathrm{sf}}\right)/\alpha)}, \tag{8}$$

where $\dot{\sigma}_{\mathrm{df}}$ is the loading rate of the dynamic fracture and $\dot{\sigma}_{\mathrm{sf}}$ is the static fracture loading rate. In this work, the dynamic loading rate with the slowest order of magnitude is equal to the static loading rate, and α and β are constants. According to the obtained experimental data and Equation (4), α and β are 8.18 and 0.45, respectively. Based on the fitting formula, Figure 7 gives a comparison of the fitting curve and experimental data, and it can be seen that the fit is good; the fitting curve is very close to the measured data.

7. Conclusions

In this study, the fracture toughness of SCB specimens was measured at different loading rates with an INSTRON testing system and a modified SHPB system, and the mechanical properties of the marble obtained from the quasistatic and dynamic fracture tests were qualitatively and quantitatively analysed. In addition, the main results are as follows:

(1) The load-displacement curves at different loading rates were obtained, and it was noted that both the static and dynamic fracture processes can be divided into two distinct stages; the fracture forms near the inflection point between these two stages. However, owing to the high speed of the dynamic impact, the dynamic fracture displacement is clearly smaller than the displacement of the static fracture in the rock

(2) The fracture toughness under pure static conditions and a pure dynamic state was measured. It is found that both the static fracture toughness and dynamic fracture toughness are influenced by the loading rate, and the effect of the loading rate under the static load is obviously smaller than that under the dynamic one. It is also proven that the fracture toughness in a pure static state (logarithmic) increases linearly with the loading rate; hence, it can be concluded that the fracture toughness of the rock increases exponentially with the increasing loading rate

(3) A continuous function was proposed to express the relation between the rock fracture toughness and the loading rate and can better characterize the fracture toughness of rock under low to high loading rates

Data Availability

All data generated or analysed during this study are included in this published article.

Conflicts of Interest

We declare that we do not have any commercial or associative interest that represents a conflict of interest in connection with the work submitted.

Authors' Contributions

The manuscript is approved by all authors for publication.

Acknowledgments

This work was supported by the National Natural Science Foundation of China (Grant No. 41877272) and the

Fundamental Research Funds for the Central Universities (Grant No. 2242020R10023).

References

[1] M. Cai, P. K. Kaiser, Y. Tasaka, T. Maejima, H. Morioka, and M. Minami, "Generalized crack initiation and crack damage stress thresholds of brittle rock masses near underground excavations," *International Journal of Rock Mechanics and Mining Sciences*, vol. 41, no. 5, pp. 833–847, 2004.

[2] X. Wang, Z. J. Wen, Y. J. Jiang, and H. Huang, "Experimental study on mechanical and acoustic emission characteristics of rock-like material under non-uniformly distributed loads," *Rock Mechanics and Rock Engineering*, vol. 51, no. 3, pp. 729–745, 2018.

[3] Q. Jiang, X. T. Feng, Y. L. Fan et al., "In situ experimental investigation of basalt spalling in a large underground powerhouse cavern," *Tunnelling and Underground Space Technology*, vol. 68, pp. 82–94, 2017.

[4] F. Q. Gong, Y. Luo, X. B. Li, X. F. Si, and M. Tao, "Experimental simulation investigation on rockburst induced by spalling failure in deep circular tunnels," *Tunnelling and Underground Space Technology*, vol. 81, pp. 413–427, 2018.

[5] F. Q. Gong, W. X. Wu, T. B. Li, and X. F. Si, "Experimental simulation and investigation of spalling failure of rectangular tunnel under different three-dimensional stress states," *International Journal of Rock Mechanics and Mining Sciences*, vol. 122, article 104081, 2019.

[6] F. Q. Gong, X. F. Si, X. B. Li, and S. Y. Wang, "Experimental investigation of strain rockburst in circular caverns under deep three-dimensional high-stress conditions," *Rock Mechanics and Rock Engineering*, vol. 52, no. 5, pp. 1459–1474, 2019.

[7] X. J. Hao, L. Yuan, J. Xue et al., "Physical model test and evaluation for the tunnel stability influenced by magnitude and path of loading," *Journal of Testing and Evaluation*, vol. 48, no. 2, 2020.

[8] C. Wu, F. Q. Gong, and Y. Luo, "A new quantitative method to identify the crack damage stress of rock using AE detection parameters," *Bulletin of Engineering Geology and the Environment*, 2020.

[9] F. Z. Meng, L. N. Y. Wong, H. Zhou, Z. Q. Wang, and L. M. Zhang, "Asperity degradation characteristics of soft rock-like fractures under shearing based on acoustic emission monitoring," *Engineering Geology*, vol. 266, no. 5, article 105392, 2020.

[10] X. F. Si and F. Q. Gong, "Strength-weakening effect and shear-tension failure mode transformation mechanism of rockburst for fine-grained granite under triaxial unloading compression," *International Journal of Rock Mechanics and Mining Sciences*, vol. 131, article 104347, 2020.

[11] M. D. Wei, F. Dai, N. W. Xu, T. Zhao, and K. W. Xia, "Experimental and numerical study on the fracture process zone and fracture toughness determination for ISRM-suggested semi-circular bend rock specimen," *Engineering Fracture Mechanics*, vol. 154, pp. 43–56, 2016.

[12] F. Q. Gong, S. Luo, and J. Y. Yan, "Energy storage and dissipation evolution process and characteristics of marble in three tension-type failure tests," *Rock Mechanics and Rock Engineering*, vol. 51, no. 11, pp. 3613–3624, 2018.

[13] S. Luo and F. Q. Gong, "Linear energy storage and dissipation laws during rock fracture under three-point flexural loading," *Engineering Fracture Mechanics*, vol. 234, article 107102, 2020.

[14] M. Z. Gao, R. Zhang, J. Xie, G. Y. Peng, B. Yu, and P. G. Ranjith, "Field experiments on fracture evolution and correlations between connectivity and abutment pressure under top coal caving conditions," *International Journal of Rock Mechanics and Mining Sciences*, vol. 111, pp. 84–93, 2018.

[15] M. R. Ayatollahi and J. Akbardoost, "Size and geometry effects on rock fracture toughness: mode I fracture," *Rock Mechanics and Rock Engineering*, vol. 47, pp. 677–687, 2014.

[16] M. R. M. Aliha and A. Bahmani, "Rock fracture toughness study under mixed mode I/III loading," *Rock Mechanics and Rock Engineering*, vol. 50, no. 7, pp. 1739–1751, 2017.

[17] K. Peng, H. Lv, F. Z. Yan, Q. L. Zou, X. Song, and Z. P. Liu, "Effects of temperature on mechanical properties of granite under different fracture modes," *Engineering Fracture Mechanics*, vol. 226, article 106838, 2020.

[18] F. Ouchterlony, "Suggested methods for determining the fracture toughness of rock," *International Journal of Rock Mechanics and Mining Sciences & Geomechanics Abstracts*, vol. 25, no. 2, pp. 71–96, 1988.

[19] R. J. Fowell, "Suggested method for determining mode I fracture toughness using cracked chevron notched Brazilian disc (CCNBD) specimens," *International Journal of Rock Mechanics and Mining Sciences & Geomechanics Abstracts*, vol. 32, no. 1, pp. 57–64, 1995.

[20] M. D. Kuruppu, "Fracture toughness measurement using chevron notched semi-circular bend specimen," *International journal of fracture*, vol. 86, no. 4, pp. L33–L38, 1997.

[21] H. Guo, N. I. Aziz, and L. C. Schmidt, "Rock fracture toughness determination by the Brazilian test," *Engineering Geology*, vol. 33, no. 3, pp. 177–188, 1993.

[22] C. Atkinson, R. E. Smelser, and J. Sanchez, "Combined mode fracture via the cracked Brazilian disk test," *International Journal of Fracture*, vol. 18, no. 4, pp. 279–291, 1982.

[23] R. J. Fowell and C. Xu, "The use of the cracked Brazilian disc geometry for rock fracture investigations," *International Journal of Rock Mechanics and Mining Sciences & Geomechanics Abstracts*, vol. 31, no. 6, pp. 571–579, 1994.

[24] K. P. Chong and M. D. Kuruppu, "New specimen for fracture–toughness determination for rock and other materials," *International Journal of Fracture*, vol. 26, no. 2, pp. R59–R62, 1984.

[25] M. D. Kuruppu, Y. Obara, M. R. Ayatollahi, K. P. Chong, and T. Funatsu, "ISRM-suggested method for determining the mode I static fracture toughness using semi-circular bend specimen," *Rock Mechanics and Rock Engineering*, vol. 47, no. 1, pp. 267–274, 2014.

[26] Y. X. Zhou, K. Xia, X. B. Li et al., "Suggested methods for determining the dynamic strength parameters and mode-I fracture toughness of rock materials," *International Journal of Rock Mechanics and Mining Sciences*, vol. 49, pp. 105–112, 2012.

[27] Z. X. Zhang, S. Q. Kou, J. Yu, Y. Yu, L. G. Jiang, and P.-A. Lindqvist, "Effects of loading rate on rock fracture," *International Journal of Rock Mechanics and Mining Sciences*, vol. 36, no. 5, pp. 597–611, 1999.

[28] L. Zhou, Z. M. Zhu, H. Qiu, X. S. Zhang, and L. Lang, "Study of the effect of loading rates on crack propagation velocity and rock fracture toughness using cracked tunnel specimens," *International Journal of Rock Mechanics and Mining Sciences*, vol. 112, pp. 25–34, 2018.

[29] Q. Z. Wang, S. Zhang, and H. P. Xie, "Rock dynamic fracture toughness tested with holed-cracked flattened Brazilian discs

diametrically impacted by SHPB and its size effect," *Experimental Mechanics*, vol. 50, no. 7, pp. 877–885, 2010.

[30] F. Dai, R. Chen, and K. W. Xia, "A semi-circular bend technique for determining dynamic fracture toughness," *Experimental Mechanics*, vol. 50, no. 6, pp. 783–791, 2010.

[31] Q. B. Zhang and J. Zhao, "Effect of loading rate on fracture toughness and failure micromechanisms in marble," *Engineering Fracture Mechanics*, vol. 102, pp. 288–309, 2013.

[32] T. Backers, N. Fardin, G. Dresen, and O. Stephansson, "Effect of loading rate on mode I fracture toughness, roughness and micromechanics of sandstone," *International Journal of Rock Mechanics and Mining Sciences*, vol. 40, no. 3, pp. 425–433, 2003.

[33] F. Q. Gong, H. Ye, and Y. Luo, "The effect of high loading rate on the behaviour and mechanical properties of coal-rock combined body," *Shock and Vibration*, vol. 2018, Article ID 4374530, 9 pages, 2018.

[34] X. F. Si, F. Q. Gong, X. B. Li, S. Y. Wang, and S. Luo, "Dynamic Mohr–Coulomb and Hoek–Brown strength criteria of sandstone at high strain rates," *International Journal of Rock Mechanics and Mining Sciences*, vol. 115, pp. 48–59, 2019.

[35] Y. Xu, F. Dai, N. W. Xu, and T. Zhao, "Numerical investigation of dynamic rock fracture toughness determination using a semi-circular bend specimen in split Hopkinson pressure bar testing," *Rock Mechanics and Rock Engineering*, vol. 49, no. 3, pp. 731–745, 2016.

[36] J. B. Zhu, Z. Y. Liao, and C. A. Tang, "Numerical SHPB tests of rocks under combined static and dynamic loading conditions with application to dynamic behavior of rocks under in situ stresses," *Rock Mechanics and Rock Engineering*, vol. 49, no. 10, pp. 3935–3946, 2016.

[37] F. Q. Gong, X. F. Si, X. B. Li, and S. Y. Wang, "Dynamic triaxial compression tests on sandstone at high strain rates and low confining pressures with split Hopkinson pressure bar," *International Journal of Rock Mechanics and Mining Sciences*, vol. 113, pp. 211–219, 2019.

[38] F. Q. Gong and J. Hu, "Energy dissipation characteristic of red sandstone in the dynamic Brazilian disc test with SHPB setup," *Advances in Civil Engineering*, vol. 2020, Article ID 7160937, 10 pages, 2020.

[39] D. J. Frew, M. J. Forrestal, and W. Chen, "A split Hopkinson pressure bar technique to determine compressive stress–strain data for rock materials," *Experimental Mechanics*, vol. 41, no. 1, pp. 40–46, 2001.

[40] X. B. Li, T. S. Lok, and J. Zhao, "Dynamic characteristics of granite subjected to intermediate loading rate," *Rock Mechanics and Rock Engineering*, vol. 38, no. 1, pp. 21–39, 2005.

[41] Q. B. Zhang and J. Zhao, "Determination of mechanical properties and full-field strain measurements of rock material under dynamic loads," *International Journal of Rock Mechanics and Mining Sciences*, vol. 60, pp. 423–439, 2013.

[42] C. Huang, G. Subhash, and S. J. Vitton, "A dynamic damage growth model for uniaxial compressive response of rock aggregates," *Mechanics of Materials*, vol. 34, no. 5, pp. 267–277, 2002.

[43] F. Q. Gong and G. F. Zhao, "Dynamic indirect tensile strength of sandstone under different loading rates," *Rock Mechanics and Rock Engineering*, vol. 47, no. 6, pp. 2271–2278, 2014.